International Journal of Environmental Science and Technology (2023) 20:11865–11876
https://doi.org/10.1007/s13762-023-04771-6

ORIGINAL PAPER

Enhanced photocatalytic activity of Fe-, S- and N-codoped TiO_2 for sulfadiazine degradation

X. Xin[1] · H. Liu[2] · J. Sun[2] · K. Gao[2] · R. Jia[1,2]

Received: 23 September 2022 / Revised: 26 December 2022 / Accepted: 7 January 2023 / Published online: 18 January 2023

Abstract
The composite material based on *N*-, *S*-, and Fe-doped TiO_2 (NSFe-TiO_2) synthesized by wet impregnation was used as a photocatalyst to rapidly degrade sulfadiazine. The photocatalytic degradation behavior and mechanism of sulfadiazine on NSFe-TiO_2 were investigated for revealing the role of degradation under ultraviolet light. The results showed that compared with TiO_2, NSFe-TiO_2 markedly improved the efficiency in photocatalytic degradation of sulfadiazine: more than 90% of sulfadiazine could be removed within 120 min by NSFe-TiO_2 dosage of 20 mg L^{-1}. The process conformed to first-order reaction kinetics model. The parameters such as loaded amount of NSFe-TiO_2, solution pH value, humic acid concentration and recycle numbers on removal efficiency were also studied. Compared to neutral and alkaline conditions, acidic condition was not conducive to the photocatalysis. HA, Ca^{2+}, Cu^{2+} and Zn^{2+} in the actual water body had mild inhibition on sulfadiazine degradation in UV/NSFe-TiO_2 system. Fragments screened by high-resolution mass spectrometry were conducted to explore the oxidation mechanism and pathways of sulfadiazine degradation. On the whole, UV/NSFe-TiO_2 photocatalysis has a good effect on sulfadiazine removal.

Keywords Sulfadiazine · Antibiotics · NSFe-TiO_2 · Photocatalysis · Degradation mechanism

Introduction

Nowadays, many scientists focus their attention on solving the environment problems using green technologies, materials, methods of water treatment. In recent years, high attention has been paid to the problem of new pollutants in aquatic environment, such as persistent organic pollutants (POPs), endocrine disruption chemicals (EDCs) and antibiotics class (Knidri et al. 2018; Sarode et al. 2019; Kumara et al. 2022; Metcalfe et al. 2022), which has become highly relevant.

In the past two years, the use of antibiotics worldwide has increased rapidly due to the COVID-19 outbreak (Guan et al. 2020; Chen et al. 2021). However, at present, there is no comprehensive picture of antimicrobial use in this outbreak, and it is hardly to quantify the level of contamination in the entire environment. Even so, the environmental pollution caused by antibiotics has attracted people's attention. Antibiotics may cause some adverse effects to aquatic microorganisms or even to human's health and one of their most important effects is that they promote the increase in important resistant genes and bacteria (Michael et al. 2013).

Sulfonamides exhibit high solubility, long persistence and high mobility in water (Yadav et al. 2018) leading to high residual concentrations in water environment, for example, wastewater after processing, source water, river water and ground water (Xu et al. 2007; Chang et al. 2010; Chen and Zhou 2014; García-Galan et al. 2010; Zhang et al. 2015), which could threaten the ecosystem and human health (Baran et al. 2011). It should be noted sulfadiazine is partially removed in wastewater treatment plant (Yadav et al. 2018) and the effluent from the secondary sedimentation tank often contains a large number of sulfonamides and other drugs (Pan et al. 2014). For the sake of effectively eliminating the sulfonamides in water, different treatments available have been researched and applied, such as adsorption (Li et al. 2019), membrane filtration (Shamsuddin et al.

Editorial responsibility: Chongqing Wang.

✉ R. Jia
jiaruibao1968@163.com

1 Shandong Province Water Supply and Drainage Monitoring Center, Jinan 250101, China

2 School of Water Conservancy and Environment, University of Jinan, Jinan 250022, China

2015; Hollman et al. 2020) and biological treatment (Edefell et al. 2021). Although various physicochemical and biological technologies can be used to remove these refractory compounds, most physicochemical methods merely transfer contaminants from the aqueous phase to the solid phase without complete degradation or mineralization (Manjunath et al. 2017). Researchers have been looking for greener and more efficient technologies. Photocatalysis is a high-efficiency, low-cost and environment-friendly advanced technology, which can realize the mineralization of antibiotics and form small molecules with low toxicity (Tab et al. 2020; Wang et al. 2020). Among many photocatalysts, TiO_2 is widely used catalyst due to its high photostability, hypotoxicity and low cost (Eleftheriadou et al. 2019). TiO_2 photocatalysis using ultraviolet (UV) light has been widely studied and shown to degrade sulfadiazine effectively (Cui et al. 2016).

Fe salt as a catalyst is known as an advanced, economical and highly efficient way to treat organic pollutant (Shi et al. 2022; Maryam et al. 2022; He et al. 2022). The difficult recovery of Fe salt from effluents limits its application in water treatment (Leal et al. 2018). The immobilization of iron on the supports could solve the problem (Bedia et al. 2017). Fe^{3+} self-loading technology as one of the means to enhance the photocatalytic effect of TiO_2 has shown unique charm (Baran et al. 2009b), which is achieved by improving the separation of the TiO_2 electron hole, while the recovery of Fe^{3+} and the photocatalyst severely restrict the development of the technology (Baran et al. 2009a).

In addition, the loading of *S* and *N* forming Fe–*S* and Fe–*N* species is believed to display such synergistic effect in the improvement in catalytic activity. Researches show that Fe and S complexes on the catalyst surface could facilitate the electron transfer oxidant and iron oxide at the photocatalysts interface (Cheng et al. 2016). The introduction of N onto the surface of Fe/TiO_2 leads to the formation of Fe–N_x coordinated active sites. On the other hand, the *S* or *N* dopants also form *S*-containing or *N*-containing groups on the TiO_2 surface, which is favorable to the enhancement of catalytic activity. Yao et al. reported the dopants of metal and N generated new active sites on the carbon surface and promoted the donor–acceptor properties, which led to the improvement in the interfacial electron transfer (Yao et al. 2016). Yang et al. reported that the pyridinic *N* and pyrrolic *N* could strengthen the dispersion between phenol and the basal plane of activated carbon (Yang et al. 2014).

In this work, functional TiO_2 (NSFe-TiO_2) was prepared by an immersion method using ammonium ferrous sulfate as precursor. NSFe-TiO_2 was characterized by scanning electron microscope with electron dispersive spectroscopy (SEM–EDS), *X*-ray diffraction patterns (XRD), *X*-ray photoelectron spectroscopy (XPS), FT–IR and UV–vis diffuse reflectance spectra (UV–vis DRS). The photocatalytic performance of NSFe-TiO_2 to sulfadiazine was investigated under UV irradiation. The effectiveness of sulfadiazine under different experimental variables, such as NSFe-TiO_2 concentration, solution pH, humic acid (HA) and natural inorganic materials, was also explored. The possible pathways of sulfadiazine photocatalysis by UV/ NSFe-TiO_2 were proposed based on the sulfadiazine degradation intermediates identified by high-performance liquid chromatography–time of flight mass spectrometry (HPLC-QTOF). Based on these results, this study aims to evaluate the photocatalytic potential of NSFe-TiO_2 for sulfadiazine and provide a scientific basis for the environmental application of water/wastewater treatment.

Materials and methods

Materials

TiO_2 (anatase, > 99.5%) and standard sulfadiazine were obtained from Aladdin Chemistry Co. Ltd (China). Methanol was purchased from Merck (Germany). Other chemicals and reagents were purchased from Sinopharm Chemical Reagent Co., Ltd (China). All solutions were prepared in deionized water (18.2 Ω/cm) using a purification machine (Millipore, Billerica, MA).

Preparation and characterization of catalysts

This synthesis method is based on Yang et al.'s study (Yang et al. 2020). 1 L 0.2 mol/L of ammonium ferrous sulfate was prepared with deionized water and used to synthesize Fe-, S- and N-codoped TiO_2 (NSFe-TiO_2). 2 g TiO_2 was immersed with the above solution and dried at 150 °C, and these catalysts were roasted in a tube furnace at 450 °C for 5 h. After grinding, the catalytic material NSFe-TiO_2 was obtained.

Scanning electron microscope (SEM–EDS, FEI Quanta FEG 250, USA) was used to observe the morphological structure and dispersion of NSFe-TiO_2. *X*-ray diffraction patterns (XRD) were acquired with an *X*-ray diffractometer with Cu-*K*α radiation ($\lambda = 0.154$ nm) at 40 kV/30 mA and a scan rate of 1°/sec and with 2θ range from 5 to 70° (Bruker/D8 ADVANCE). *X*-ray photoelectron spectroscopy (XPS, Bruker S8 TIGER, Germany) was carried out in an ultrahigh vacuum system. The zeta potential was measured at various pH with a Zetasizer Nano ZS90 (Malvern Instrument, UK). The optical properties of as-synthetized catalysts were probed by measuring their UV–vis DRS (Varian Cary 500 Scan S4800, USA).

Catalytic activity tests

Photocatalytic experiments were carried out in photochemical reactor (BL-GHX-V, Shanghai BiLon Instrument Co., Ltd., China). In a typical batch experiment, the as-prepared NSFe-TiO_2 was added into 100 mL of sulfadiazine solution containing (10 μg/L) and was stirred for 30 min in the dark in order to reach adsorption equilibrium on the catalysts' surface. A magnetic stirring apparatus was used to keep the reactor contents homogenously and the catalyst in suspension. The UV lamps ($\lambda = 365$ nm) were used in all photocatalytic experiments, and the UV intensity was measured to be 1.44 mW/cm^{-2}. After initiating the irradiance, aliquots were withdrawn from the reactor, filtered on syringe nylon membrane filters (0.2 μm pore-size) and proceeded to analysis for the determination of antibiotics concentration. Each experiment was duplicated under identical conditions.

The sulfadiazine removal (R_{SD}) was calculated as follows:

$$R_{SD} = \frac{c_0 - c_t}{c_0} \times 100\% \quad (1)$$

where c_0 is the initial concentration of sulfadiazine and c_t is the concentration of sulfadiazine at reaction time t (min).

First-order kinetic model (Eq. 2) was as follows:

$$\ln\frac{c_0}{c_t} = k_1 t \quad (2)$$

where k_1 is the observed first-order rate constant (min^{-1}), t is the photocatalytic time (min), c_0 is the concentration before photocatalysis (μg/L) and c_t is the concentration at t photocatalytic time (μg/L).

Analytical methods

Ultra-performance liquid chromatography (UPLC)-triple quadrupole mass spectrometry (Waters Xevo TQs, USA) with a chromatographic column (BEH C18, 1.7 μm, 2.1 × 50 mm, Waters ACQUITY UPLC) was used to determine the concentration of sulfadiazine. Positive polarity mode with electrospray ionization was used for sulfadiazine determination. The column temperature was maintained at 30 °C. The mobile phase was a mixture of 2:8 deionized water (0.5% formic acid) / acetonitrile (0.5% formic acid) (v/v) with flow rate of 0.30 mL/min.

Sulfadiazine degradation product analysis was conducted using UPLC/QTOF (Waters Xevo G2 QTOF, USA) with a chromatographic column (BEH C18, 1.7 μm, 2.1 × 50 mm, Waters ACQUITY UPLC). Accurate MS^E mode was used

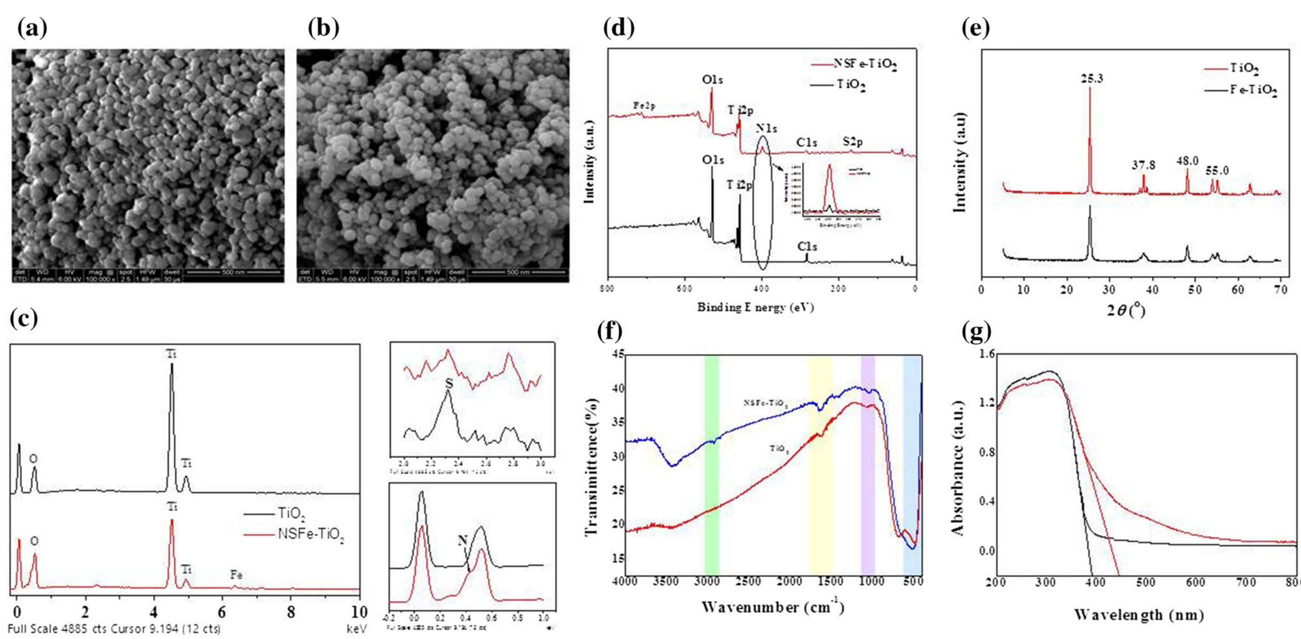

Fig. 1 Characterization of NSFe-TiO_2 and TiO_2 (**a** and **b**: SEM of NSFe-TiO_2 and TiO_2; **c**: EDS; **d**: XPS; **e**: XRD; **f**: FT-IR; **g**: DRS)

to analyze sulfadiazine and the degradation products with a scan range of 50–650 m/z.

Results and discussion

Catalyst characterization

SEM–EDS is the tool for the investigation of the surface properties The SEM images and EDS patterns for the pure TiO_2 and NSFe-TiO_2 samples are shown in Fig. 1a, b. We can see from Fig. 1a b that TiO_2 and NSFe-TiO_2 were roughly spherical and has a size range of 40 – 50 nm. Compared with the pure TiO_2, the structure of NSFe-TiO_2 has not changed, whereas it seemed doping had made the sample compact or agglomerated. To evaluate the chemical composition of the NSFe-TiO_2 composite, element mapping was performed by energy-dispersive spectroscopy (EDS) analysis and the resultant mapping images are shown in Fig. 1c. A uniform distribution of *N*, *S*, Ti, and *O* elements is observed in the NSFe-TiO_2 composite. It should be noted that weak scanning signals were observed for *S* and *N* elements due to its low concentration in the NSFe-TiO_2 composite. EDS analysis confirmed the presence of Fe, *N* and *S* in NSFe-TiO_2 samples.

The XPS spectra for the pure TiO_2 and NSFe-TiO_2 samples are shown in Fig. 1d. For pure TiO_2, the peak of binding energy at about 528.5 eV and 457.4 eV was corresponding to the O1s and Ti_2p. For NSFe-TiO_2, besides the peaks of O_1s and Ti_2p, the peak of binding energy at about 710.6 eV, 398.8 eV and 169 eV was corresponding to the Fe_2p, N_1s and S_2p. The elements of samples were determined by XPS, as shown in Table S1. The NSFe-TiO_2 had 3.62%, 1.67% and 2.63% of Fe, N and S species detected compared with TiO_2, indicating the above three species were introduced onto the TiO_2 surface.

XRD is used to measure the catalyst phase structure. The XRD patterns of composite are illustrated in Fig. 1e. As seen from this figure, XRD analysis of the pure TiO_2 and NSFe-TiO_2 samples showed that they had a well crystallized monophase structure of anatase phase (Shymanovska et al. 2022; Kanjana et al. 2021). Four peaks at 25.3°, 37.8, 48.0° and 55.0° were obtained for pure TiO_2 and NSFe-TiO_2 corresponding to (101), (004), (200) and (211) plane diffraction of anatase TiO_2 (JCPDS No. 21–1272) in the XRD graph, respectively. The crystallite sizes of pure TiO_2 and NSFe-TiO_2 were estimated by means of the Debye–Scherrer's formula (Eq. 3):

$$d = \frac{0.9\lambda}{B\cos\theta} \quad (3)$$

where λ is the *X*-ray wavelength corresponding to Cu-*K*α radiation (0.154 nm), θ is the diffraction angle and *B* is the line broadening (in radians) at half of its maximum. Average crystallite sizes of pure TiO_2 and NSFe-TiO_2 were 15.1 nm and 52.6 nm.

Figure 1f displays the FTIR spectra of TiO_2 and NSFe–TiO_2 in the 400 to 4000 cm^{-1} region. Based on the previous study (Naghibi et al 2013; Gharagozlou and Naghibi 2015), the characteristic absorption band of TiO_2 at 400–600 cm^{-1} is attributed to Ti–*O* bond. The traces of this bond could be found in TiO_2 and NSFe–TiO_2. The bending vibration of the *H–O–H* molecule is represented by the small peak at 1648 cm^{-1} (Alkorbi et al. 2022). The presence of hydroxyl group on the catalysts' surface played a significant role in improving the photocatalytic activity of the photocatalyst. Moreover, the peaks at about 2920 and 2850 cm^{-1} in the NSFe–TiO_2 FTIR spectra were attributed to sulfurous functional groups (Yuan et al. 2018). The small band around 1017 cm^{-1} is caused by stretching vibrations of the Ti-*N*-Ti bond, which clearly demonstrates that nitrogen is substitutionally doped into the TiO_2 lattice (Divya et al. 2022).

Finally, the optical properties of TiO_2 and NSFe–TiO_2 were probed by measuring their UV–vis DRS, and the results of this check are presented in Fig. 1g. In particular, when the *N*, *S* and Fe element was impregnated onto the TiO_2 powder, the absorption peak of NSFe–TiO_2 was a bathochromic shift (red shift). Notably, the edge absorbance value of the bare TiO_2 powder was calculated to be 390 nm, and that of NSFe–TiO_2 was calculated to be 442 nm. However, when the band gap energy was calculated from the measured values through Kubelka–Munk theory, the band gap energy of bare TiO_2 and NSFe–TiO_2 was calculated to be 3.18 and 3.02 eV, respectively. It was also found that the band gap energy of bare TiO_2 powder coincided with a commonly known value, and the band gap energy of NSFe–TiO_2 was lower than that of bare TiO_2 powder. UV–vis DRS analysis displayed that N, S and Fe co-doping can reduce the band gap of the involved catalysts, leading to improvement in light absorption.

Catalytic activity

Comparison of different degradation techniques

The evolution of sulfadiazine removal over different degradation techniques (UV/NSFe-TiO_2, UV/H_2O_2, UV/TiO_2,

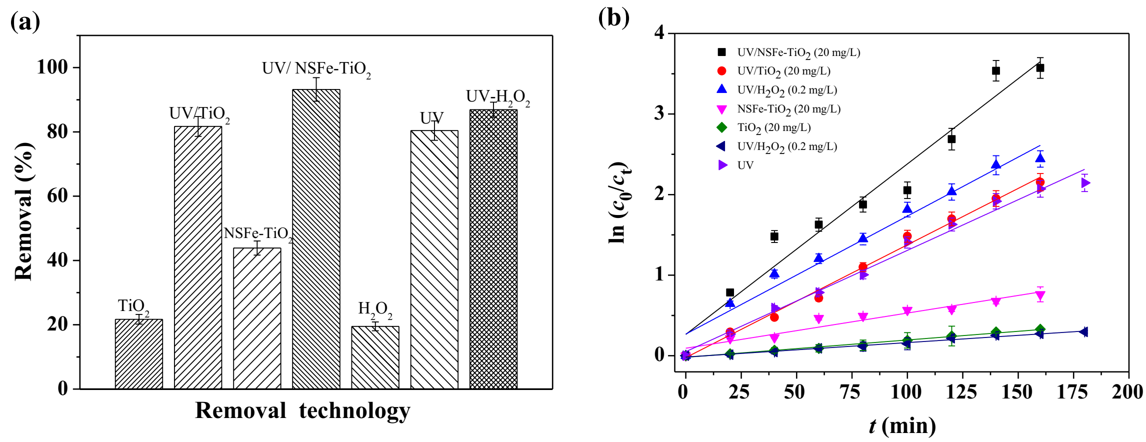

Fig. 2 Sulfadiazine removal by different removal technology. (**a**: SDM removal efficiencies using UV/NSFe-TiO_2, UV/H_2O_2, UV/TiO_2, UV photolysis, NSFe-TiO_2, TiO_2 and H_2O_2 after 120 min treatment; **b**: first-order kinetic fitting using above technologies)

UV) is shown in Fig. 2. Considering the alone oxidation of H_2O_2 and the adsorption ability of TiO_2 and NSFe-TiO_2, the contribution of oxidation with H_2O_2 (0.2 mg/L) alone and pure adsorption with TiO_2 (20 mg/L) and NSFe-TiO_2 (20 mg/L) to the removal of sulfadiazine was also evaluated.

As shown in Fig. 2, sulfadiazine can be significantly removed by UV/NSFe-TiO_2 (20 mg/L) and UV/H_2O_2 (20 mg/L). The R_{SD} was about 20% by adsorption with TiO_2 and oxidation with H_2O_2 alone, which was lower than that of NSFe-TiO_2. The R_{SD} was about 45% by adsorption with NSFe-TiO_2, higher than adsorption with TiO_2 and oxidation with H_2O_2 alone, that of NSFe-TiO_2, which indicated that adsorption effect of NSFe-TiO_2 is better than TiO_2 and H_2O_2 alone had little effect on sulfadiazine oxidation. Experimental results showed that direct photolysis, UV/H_2O_2 and UV/TiO_2 system had an ideal effect on sulfadiazine degradation with removal efficiencies of nearly 80.4%, 86.9% and 81.7%, and first-order kinetics constants of 0.0125 min^{-1}, 0.0146 min^{-1} and 0.0140 min^{-1}. It was surprising that UV/NSFe-TiO_2 showed the better processing capacity of sulfadiazine with the high removal efficiency of 93.2% and kinetics constant of 0.0216 min^{-1}, compared with UV/TiO_2 and UV homogeneous advanced oxidation such as UV/H_2O_2. In summary, by comparing the removal efficiency and removal rate, the comparative results of technological advantages are as follows: UV/NSFe-TiO_2 > UV/H_2O_2 > UV/TiO_2 > UV photolysis > NSFe-TiO_2 > TiO_2 > H_2O_2. Besides, the related results comparison of various studies on sulfadiazine photocatalytic degradation using TiO_2 is shown in Table 1. It can be seen that UV/NSFe-TiO_2 in this study has a good effect and advantage on the removal of sulfadiazine with low concentration.

Optimization of catalyst dosage

The degradation of sulfadiazine was slower by UV. After adding NSFe-TiO_2, the removal efficiency and rate were both

Table 1 Comparison of related studies on sulfadiazine photodegradation using TiO_2

Systems	Catalyst dosage (g/L)	Initial concentration (mg/L)	UV-irradiation parameters	Time (min)	Removal (%)	Reference
Bi_2O_3-TiO_2/ PAC	0.2	20	300 W Xenon lamp	30	72	Wang, et al 2020
TiO_2/ZEO	1.0	10	20 W UV lamp (λ_{max} = 265 nm)	120	90	Liu, et al 2018
Degussa P25 TiO_2	1.0	10	300 W Xenon lamp with the filters (λ = 475, 420, 365 and 254 nm)	60	29%, 52%, 99%, 94%	Li, et al 2021
C, N-TiO_2@C	1.0	1.0–20 mg/L	160 W high-pressure mercury lamp	140	99.25	Li, et al 2022
BC_TiO_2_MagEx	0.1	5	The lamp with 55 Wm^{-2} (290–400 nm)	240	76	Silva et al. (2021)
NSFe-TiO_2	0.02	0.01	UV lamps (λ = 365 nm)	120	93.2	This study

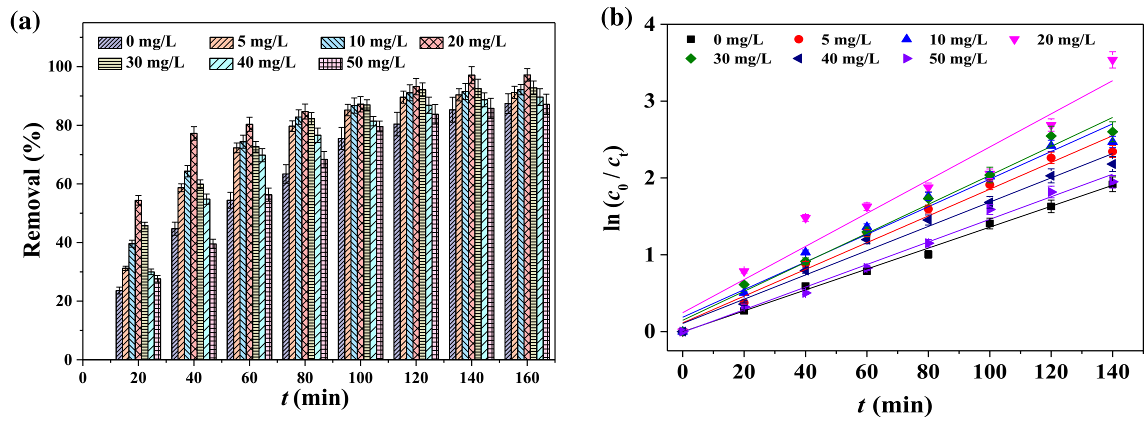

Fig. 3 Optimization of catalyst dosage. (**a**: removal efficiencies using various concentrations of catalysts at different reaction times; **b**: first-order kinetic fitting of sulfadiazine removal using various catalysts concentrations)

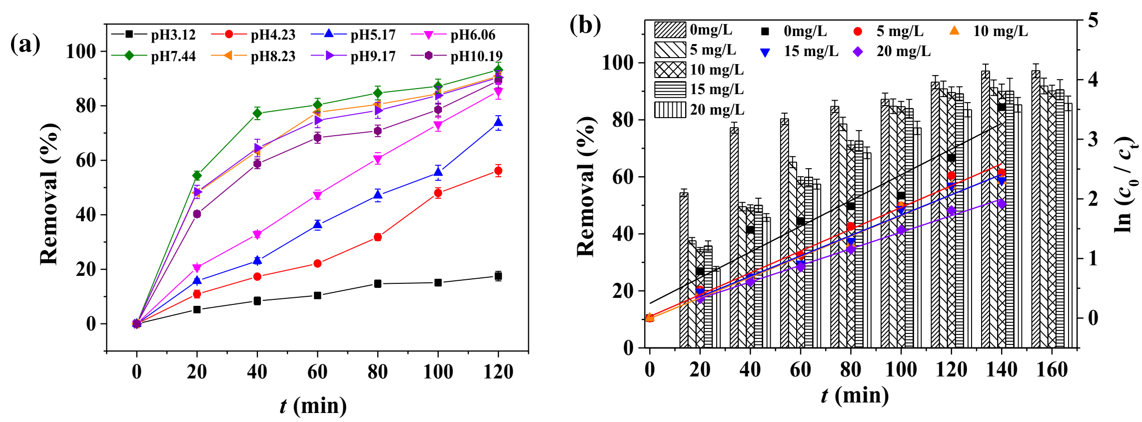

Fig. 4 (**a**) Effect of pH on sulfadiazine degradation in UV/NSFe-TiO_2 system. (**b**) Effect of HA on removal efficiencies (column) and first-order kinetic fitting (line)

improved. With the increase in catalyst dosage from 5 to 20 mg/L, the degradation effect and degradation rate were also increased. The removal of sulfadiazine onto NSFe-TiO_2 was reached maximum of 93.2% with the NSFe-TiO_2 concentration of 20 mg/L. And then, the removal decreased with NSFe-TiO_2 concentration increasing due to the increase in turbidity in the reaction system which could cause scattering and absorption of UV light and aggregation of the catalyst particles (Koltsakidou et al. 2017).

The sulfadiazine removal by UV/NSFe-TiO_2 photocatalysis conformed to the first-order kinetics, which is shown in Fig. 3b and Table S2. NSFe-TiO_2 photocatalysis followed first-order reaction kinetics ($R^2 > 0.90$). It was worth noting that at catalyst dosages of 10–30 mg/L, the k_1 values were high. At the dosage of 20 mg/L, the sulfadiazine removal rate (0.0216 min^{-1}) was 1.6 times higher to UV system.

Effect of pH

The solution pH played an important role in sulfadiazine degradation in UV/NSFe-TiO_2 system, as illustrated in Fig. 4a. Figure 4a clearly indicates that the studied system possessed a different photocatalytic efficiency for sulfadiazine degradation within pH range of 4–10, and the sulfadiazine degradation was promoted along with the increase in pH from 3 to 7 and then decreased slowly with the increase in pH from 7 to 10. The removal efficiencies at acidic conditions (pH 3–6) were lower than that at neutral or alkaline conditions, which demonstrated that acidic condition inhibited the photocatalytic reactions. The sulfadiazine removal increased dramatically when the initial pH maintained unadjusted (pH = 7.44).

Under acidic condition, the Fe and Ti were released, which might lead to a reduction in photocatalysis. Moreover, research showed that·OH could be quenched quickly in the presence of many H^+ ions in solution (Gao et al. 2021). The pH of zero-point charge (pH_{PZC}) of NSFe-TiO_2 was about 7, as shown in Fig. S1. The pK_{a1} and pK_{a2} values of sulfadiazine are 1.57 and 6.50, respectively. When the solution pH is 6.5–7, the surface of sulfadiazine is negatively charged or exists as a neutral molecule, which could be easily to be adsorbed on surface of NSFe-TiO_2, promoting the degradation.

Effect of natural organic materials

Humic acid (HA) is one of the photoabsorbent substances ubiquitous in natural water and plays an important role in photochemistry. Therefore, the effect of HA on sulfadiazine degradation in the study was investigated (Fig. 4b). When the concentration of HA increased (0–20 mg·L^{-1}), the removal efficiency of sulfadiazine by UV/NSFe-TiO_2 photocatalysis was reduced by 12% and rate was decreased from 0.0216 to 0.0139 min^{-1}. HA in water performed a certain inhibitory effect on sulfadiazine degradation by UV/NSFe-TiO_2 photocatalysis. This negative effect could be caused by the following two factors: (i) HA could compete with sulfadiazine for active radicals produced in UV/NSFe-TiO_2 photocatalysis (Long et al. 2016); (ii) HA could block the active sites of the catalyst NSFe-TiO_2 due to the strong π–π stacking (Chen et al. 2018).

Effect of natural inorganic materials

Studies have suggested that metal ions and some inorganic anions can affect the photolysis of the antibiotics (Möhler et al. 2017; Efthimiadou et al. 2007). The effects of inorganic anions were investigated, such as chloride, sulfate, bicarbonate and metals with varying concentrations (Table S3 for details).

To investigate the effect of metal ions on the photolysis of sulfadiazine, Ca^{2+}, Cu^{2+} and Zn^{2+} were chosen in our research. For all investigated concentrations of Ca^{2+}, Cu^{2+} C and Zn^{2+}, sulfadiazine removal was inhibited. As shown in Fig. 5 (a, b, c), with the increase in Ca^{2+}, Cu^{2+} and Zn^{2+} concentration, there was a concurrent decrease in the sulfadiazine removal efficiencies and rate. When the concentrations were 100 mg/L, 150 mg/L, 200 mg/L of Ca^{2+}, 0.5 mg/L,1.0 mg/L 1.5 mg/L of Cu^{2+} and Zn^{2+}, the removal efficiencies decreased by about 5–7% of Ca^{2+}, 9–36% of Cu^{2+} and 5–8% of Zn^{2+} in 160 min reaction time compared with no metal in pure. For the rate constants, they are also lower than that of no metal in pure (Table S4 for details).

Chloride (Cl^-), sulfate (SO_4^{2-}) and bicarbonate (HCO_3^-) were considered with different concentrations based on the amount in actual water (Fig. 5d, e, f). Sulfadiazine removal

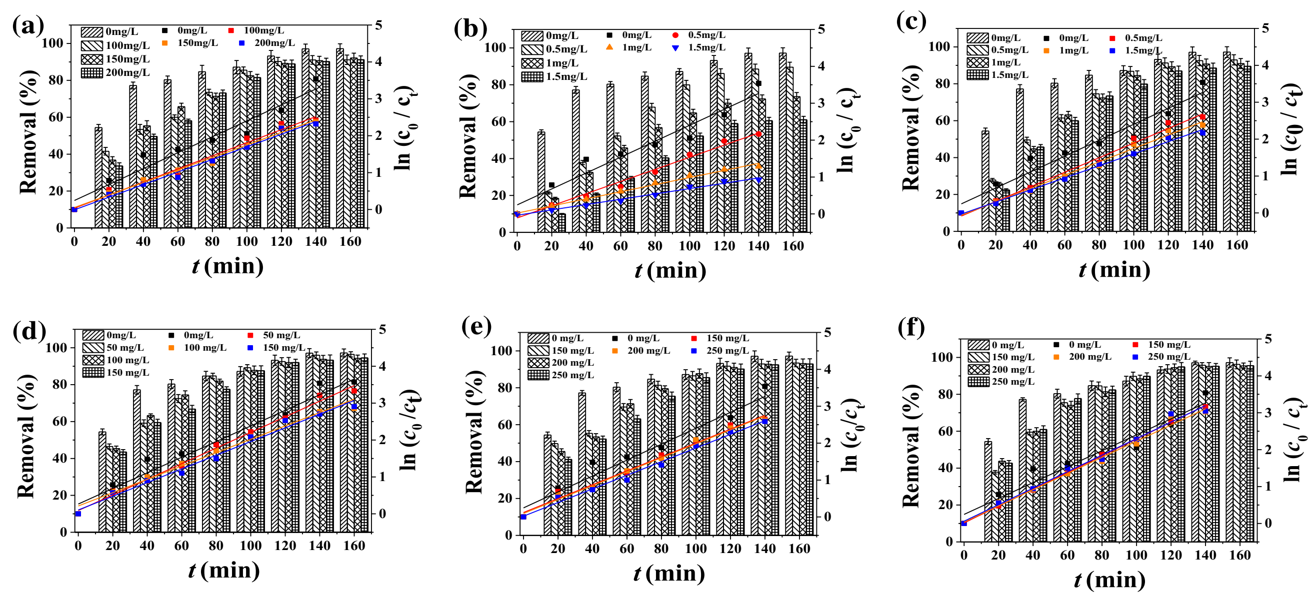

Fig. 5 Effect of inorganic materials on removal efficiencies and kinetic rate constants on degradation of sulfadiazine (a: Ca^{2+}; b: Cu^{2+}; c: Zn^{2+}; d: Cl^-; e: SO_4^{2-}; f: HCO_3^-)

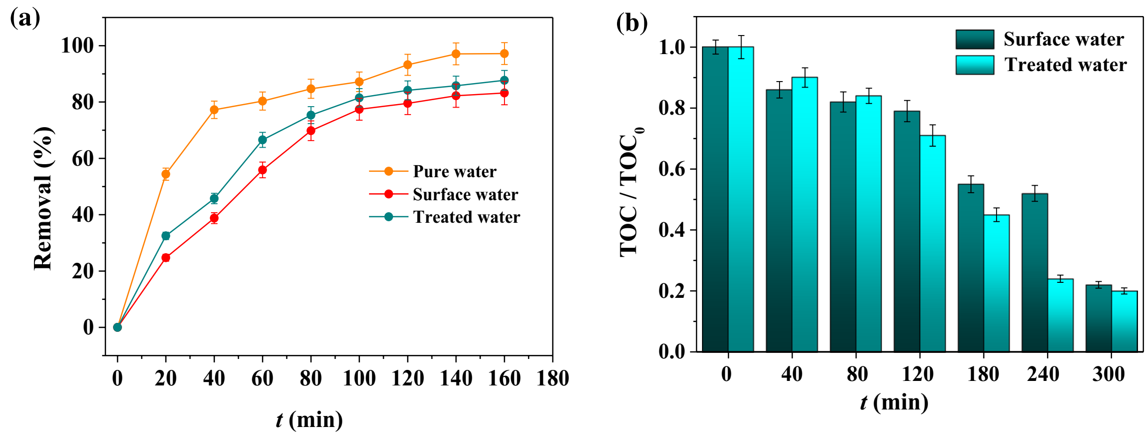

Fig. 6 Photocatalytic degradation of sulfadiazine in real water. (Experimental conditions: $c_0 = 10$ μg/L, NSFe-TiO_2: 10 μmol/L)

slightly decreased from 97.2% to about 92% with the concentrations of Cl^-, SO_4^{2-} and HCO_3^- increasing. The pH of zero-point charge (pH_{PZC}) of NSFe-TiO_2 was about 7, as shown in Fig. S1. When the solution pH is < 7, the surface of NSFe-TiO_2 is positively charged. It could easily adsorb inorganic anions, which might affect the size of catalyst and change the reactivity of NSFe-TiO_2 suspension.

Photocatalytic oxidation in actual water

In order to evaluate the application effect of NSFe-TiO_2 photocatalysis on the elimination of sulfadiazine in actual water body, experiments were carried out with surface water and treated water (drinking water produced by surface water treatment) in Jinan of China. The photocatalytic degradation of sulfadiazine is shown in Fig. 6a. The applications of photocatalysis on elimination of sulfadiazine in surface water and treated water led to lower removal efficiencies, which were reduced by 14% in surface water and 9.5% in treated water compared with achieved in pure water. This decrease in the photodegradation efficiency may be ascribed to the following two factors: (i) the presence of organic matter in surface water and treated water could form complexes with sulfadiazine as well as compete with sulfadiazine, resulting in an overall (Xiao et al. 2016; Candido et al. 2016) and (ii) the presence of inorganic ions acted as scavengers of hydroxyl radicals (Evgenidou et al. 2021).

In order to assess the overall efficiency of the process, the mineralization of the real water with 10 μg/L sulfadiazine was also investigated. The change of total organic

Fig. 7 Proposed degradation pathway of sulfadiazine

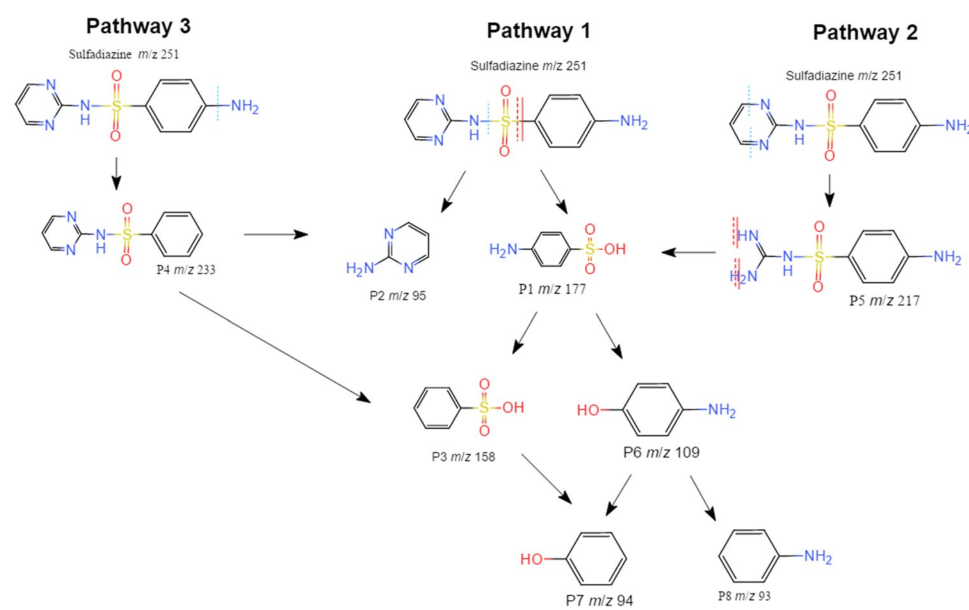

carbon (TOC) concentration was used to reflect the degree of mineralization, and the results are presented in Fig. 6b. Obviously, the reduction in TOC was not more than 20% within 80 min treatment and provoked a satisfactory reduction in the TOC (− 80%) after 5 h treatment. Prolonged treatment time could lead to complete mineralization of sulfadiazine. Overall, the following conclusions could be drawn that the photocatalytic process was effectively applied for the elimination of sulfadiazine in actual water.

SDM degradation mechanisms

The samples collected in UV/NSFe-TiO_2 photocatalysis on the elimination of sulfadiazine were analyzed by HPLC-TOFMS. The fragmentation ions with intensity greater than 1×10^4 were selected for subsequent study. The possible sulfadiazine degradation pathways were deduced based on mass-to-charge ratio (*m*/*z*) values of intermediate compounds. The possible sulfadiazine degradation pathways are depicted in Fig. 7.

In **Pathway 1**, the breakdown of S–N bond of sulfadiazine due to hydroxyl radical attack resulted in the formation of P1 (*m*/*z* 177) and P2 (*m*/*z* 95), which was also identified in Calza's study (Calza et al. 2004). In **Pathway 2**, since the carbon–nitrogen bond was unstable and vulnerable to negative charges (Rong et al. 2014), the pyrimidine ring broke to form P5 (*m*/*z* 217). P5 was attacked by hydroxyl radicals, cleaving the potential site of S–N bond and forming P1. P4 (*m*/*z* 233) in **Pathway 3** was a product of dissociation of amine group from the benzene ring. When hydroxyl radicals attack compound P4, it can be cleaved into fragments P2 or P3. There were two possible reaction pathways and products P3 (*m*/*z* 158) and P6 (*m*/*z* 109) for degradation of P1: (1) amino group on the benzene ring was cleaved to form P3; the SO_2 on the benzene ring was extruded by hydroxyl radicals attack in the formation of hydroxylated P6. Moreover, P7 (Phenol, *m*/*z* 94) was emerged due to the detachment of SO_2 from P3 and NH_2 from P6. P8 (Aniline, *m*/*z* 93) was possible products by dihydroxylation of P6.

Reusability and stability of NSFe-TiO2

The stability and reusability are key factors for long-run applications of the NSFe-TiO_2. The reusability was examined for five successive runs.

The NSFe-TiO_2 was recovered from the solution by filtration after each experiment. Then, the NSFe-TiO_2 was wash by pure water and dried in an oven at 120 °C, and the photocatalytic degradation experiment was repeated. As seen in Fig. S2, the decline in sulfadiazine removal was not significant and the sulfadiazine removal reduced by 6.5, 8.2, 10.3, 12.1% for NSFe-TiO_2, respectively. This verified the excellent stability of NSFe-TiO_2 heterostructures throughout the photocatalytic process.

Conclusion

In summary, NSFe-TiO_2 were designed and synthesized by an immersion method. Characterization results showed that *N*, *S* and Fe species have been attached to the surface of the catalysts. NSFe-TiO_2 has the great efficiency on photodegradation of sulfadiazine. The photocatalytic process of sulfadiazine fitted first-order reaction kinetics model. Compared to neutral and weakly alkaline medium, acidic condition was not conducive to the photocatalysis. HA, Ca^{2+}, Cu^{2+} and Zn^{2+} in the actual water body performed a certain inhibitory effect on sulfadiazine degradation by UV/NSFe-TiO_2. The sulfadiazine degradation products were screened, and possible pathways of sulfadiazine degradation were proposed. The possible pathways include bond cleavage, hydroxylation, as well as interaction of the byproducts. In conclusion, UV/NSFe-TiO_2 photocatalysis is efficient in the removal of sulfadiazine and other pollutants with similar structure.

Supplementary Information The online version contains supplementary material available at https://doi.org/10.1007/s13762-023-04771-6.

Acknowledgements This study was supported by National Key Research and Development Program of China (No. 2021YFC3200805) and Natural Science Foundation of Shandong Province (No. ZR2019QEE022 and ZR2021ME166).

Author contribution X.X. involved in conceptualization, methodology, data curation, writing—reviewing and editing; J.S. took part in methodology, data curation, writing—reviewing and editing; H.L. took part in data curation, writing—reviewing and editing; K.G. involved in writing—reviewing and editing; S.S. took part in methodology, resources; R.J. involved in funding acquisition, project administration.

Funding This study was supported by National Key Research and Development Program of China (No. 2021YFC3200805) and Natural Science Foundation of Shandong Province (No. ZR2019QEE022 and ZR2021ME166).

Declarations

Conflicts of interest The authors declare that they have no known competing financial interests or personal relationships that could have appeared to influence the work reported in this paper.

References

Alkorbi AS, Javed HMA, Hussain S, Latif S, Mahr MS, Mustafa MS, Alsaiari R, Alhemiary NA (2022) Solar light-driven photocatalytic degradation of methyl blue by carbon-doped TiO_2 nanoparticles. Opt Mater Amst 127:1122591–1122595. https://doi.org/10.1016/j.optmat.2022.112259

Baran W, Adamek E, Ziemiańska J, Sobczak A (2011) Effects of the presence of sulfonamides in the environment and their influence on human health. J Hazard Mater 196:1–15. https://doi.org/10.1016/j.jhazmat.2011.08.082

Baran W, Adamek E, Sobczak A, Makowski A (2009a) Photocatalytic degradation of sulfa drugs with TiO_2, Fe salts and $TiO_2/FeCl_3$ in aquatic environment—kinetics and degradation pathway. Appl Catal B Environ 90:516–525. https://doi.org/10.1016/j.apcatb.2009.04.014

Baran W, Adamek E, Sobczak A, Sochacka J (2009b) The comparison of photocatalytic activity of Fe-salts, TiO_2 and $TiO_2/FeCl_3$ during the sulfanilamide degradation process. Catal Commun 10:811–814. https://doi.org/10.1016/j.catcom.2008.12.026

Bedia J, Monsalvo VM, Rodriguez JJ, Mohedano AF (2017) Iron catalysts by chemical activation of sewage sludge with $FeCl_3$ for CWPO. Chem Eng J 318:224–230. https://doi.org/10.1016/j.cej.2016.06.096

Calza P, Medana C, Pazzi M, Baiocchi C, Pelizzetti E (2004) Photocatalytic transformations of sulphonamides on titanium dioxide. Appl Catal B Environ 53:63–69. https://doi.org/10.1016/j.apcatb.2003.09.023

Candido JP, Andrade SJ, Fonseca AL, Silva FS, Silva MRA, Kondo MM (2016) Ibuprofen removal by heterogeneous photocatalysis and ecotoxicological evaluation of the treated solutions. Environ Sci Pollut. Res 23:19911–19920. https://doi.org/10.1007/s11356-016-6947-z

Chang X, Meyer MT, Liu X, Zhao Q, Chen H, Chen JA, Shu W (2010) Determination of antibiotics in sewage from hospitals, nursery and slaughter house, wastewater treatment plant and source water in Chongqing region of three gorge reservoir in China. Environ. Pollut. 158:1444–1450. https://doi.org/10.1016/j.envpol.2009.12.034

Chen LW, Ding DH, Liu C, Cai H, Qu Y, Yang SJ, Gao Y, Cai TM (2018) Degradation of norfloxacin by $CoFe_2O_4$-GO composite coupled with peroxymonosulfate: a comparative study and mechanistic consideration. Chem Eng J 18:947–960. https://doi.org/10.1016/j.cej.2017.10.040

Chen K, Zhou JL (2014) Occurrence and behavior of antibiotics in water and sediments from the Huangpu river, Shanghai, China. Chemosphere 95:604–612. https://doi.org/10.1016/j.chemosphere.2013.09.119

Chen Z, Guo J, Jiang Y, Shao Y (2021) High concentration and high dose of disinfectants and antibiotics used during the COVID-19 pandemic threaten human health. J Environ Sci Eur 33:11. https://doi.org/10.1186/s12302-021-00456-4

Cheng X, Guo H, Zhang Y, Liu Y, Liu H, Yang Y (2016) Oxidation of 2,4-dichlorophenol by non-radical mechanism using persulfate activated by Fe/S modified carbon nanotubes. J Colloid Interf Sci 469:277–286. https://doi.org/10.1016/j.jcis.2016.01.067

Cui C, Jin L, Jiang L, Han Q, Lin K, Lu S, Zhang D, Cao G (2016) Removal of trace level amounts of twelve sulfonamides from drinking water by UV-activated peroxymonosulfate. Sci Total Environ 572:244–251. https://doi.org/10.1016/j.scitotenv.2016.07.183

Divya G, Jaishree G, Rao TS, Chippada MLVP, Lakshmi KVD, Supriya SS (2022) Improved catalytic efficiency by *N*-doped TiO_2 via sol gel under microwave irradiation: dual applications in degradation of dye and microbes. Hybrid Adv Press. https://doi.org/10.1016/j.hybadv.2022.100010

Edefell E, Falås P, Torresi E, Hagman M, Cimbritz M, Bester K, Christensson M (2021) Promoting the degradation of organic micropollutants in tertiary moving bed biofilm reactors by controlling growth and redox conditions. J Hazard Mater 414:125535. https://doi.org/10.1016/j.jhazmat.2021.125535

Efthimiadou EK, Psomas G, Sanakis Y, Katsaros N, Karaliota A (2007) Metal complexes with the quinolone antibacterial agent n-propyl-norfloxacin: synthesis, structure and bioactivity. J Inorg Biochem 101:525–535. https://doi.org/10.1016/j.jinorgbio.2006.11.020

Eleftheriadou NM, Evgenidou E, Kyzas G, Bikiaris D, Lambropoulou D (2019) Removal of antibiotics in aqueous media by using new synthesized bio-based poly (ethylene terephthalate)–TiO_2 photocatalysts. Chemosphere 234:746–755. https://doi.org/10.1016/j.chemosphere.2019.05.239

Evgenidou E, Chatzisalata Z, Tsevis A, Bourikas K, Torounidou P, Sergelidis D, Koltsakidou A, Lambropoulou DA (2021) Photocatalytic degradation of a mixture of eight antibiotics using Cu-modified TiO_2 photocatalysts: Kinetics, mineralization, antimicrobial activity elimination and disinfection. J Environ Chem Eng 9:105295. https://doi.org/10.1016/j.jece.2021.105295

Gao YJ, Zhao Q, Li YH, Li YQ, Gou JF, Cheng XW (2021) Degradation 482 of sulfamethoxazole by peroxymonosulfate activated by waste eggshell 483 supported Ag_2O-Ag nano–particles. Chem Eng J 405:126719. https://doi.org/10.1016/j.cej.2020.126719

García-Galán MJ, Garrido T, Fraile J, Ginebreda A, Díaz-Cruz MS, BarcelóD. (2010) Simultaneous occurrence of nitrates and sulfonamide antibiotics in two ground water bodies of Catalonia (Spain). J Hydrol 383:93–101. https://doi.org/10.1016/j.jhydrol.2009.06.042

Gharagozlou M, Naghibi S (2015) Preparation of vitamin B12–TiO_2 nanohybrid studied by TEM, FTIR and optical analysis techniques. Mater Sci Semicond Proc 35:166–173. https://doi.org/10.1016/j.mssp.2015.03.009

Guan WJ, Ni ZY, Hu Y (2020) Clinical characteristics of coronavirus disease 2019 in China. N Engl J Med 382:1708–1720. https://doi.org/10.1056/NEJMoa2002032

He Z, Xu X, Wang B, Lu Z, Shi D, Wu W (2022) Evaluation of iron-loaded granular activated carbon used as heterogeneous fenton catalyst for degradation of tetracycline. J Environ Manage 322:116077. https://doi.org/10.1016/j.jenvman.2022.116077

Hollman J, Khan MF, Dominic JA, Achari G (2020) Pilot-scale treatment of neutral pharmaceuticals in municipal wastewater using reverse osmosis and ozonation. J Environ Eng 146:04020121. https://doi.org/10.1061/(ASCE)EE.1943-7870.0001777

Kanjana N, Maiaugree W, Poolcharuansin P, Laokul P (2021) Synthesis and characterization of Fe-doped TiO_2 hollow spheres for dye-sensitized solar cell applications. Mat Sci Eng B 271:115311. https://doi.org/10.1016/j.mseb.2021.115311

Knidri HE, Belaabed R, Addaou A, Laajeb A, Lahsini A (2018) Extraction, chemical modification and characterization of chitin and chitosan. Int J Biol Macromol 120:1181–1189. https://doi.org/10.1016/j.ijbiomac.2018.08.139

Koltsakidou A, Antonopoulou M, Evgenidou E, Konstantinou I, Lambropoulou DA (2017) Cytarabine degradation by simulated solar assisted photocatalysis using TiO_2. Chem Eng J 316:823–831. https://doi.org/10.1016/j.cej.2017.01.132

Kumara JA, Krithiga T, Sathish S, Renita AA, Prabu D, Lokesh S, Geetha R, Namasivayam KR, Mika S (2022) Persistent organic pollutants in water resources: Fate, occurrence, characterization and risk analysis. Sci Total Environ 831(20):154808. https://doi.org/10.1016/j.scitotenv.2022.154808

Leal TW, Lourenço LA, Brandao HDL, da Silva A, de Souza SMAGU, de Souza AAU (2018) Low-cost iron-doped catalyst for phenol degradation by heterogeneous Fenton. J Hazard Mater 359:96–103. https://doi.org/10.1016/j.jhazmat.2018.07.018

Li D, Zhang N, Yuan R, Chen H, Wang F, Zhou B (2021) Effect of wavelengths on photocatalytic oxidation mechanism of ulfadiazine and sulfamethoxazole in the presence of TiO_2. J Environ Chem Eng 9:106243. https://doi.org/10.1016/j.jece.2021.106243

Li Q, Yang HY, Zhong PZ, Jiancong NJ, Yang W, Chen J, Zhang Y, Jianmin LJ (2022) Hollow *C*, *N*-TiO_2@C surface molecularly imprinted microspheres with visible light photocatalytic regeneration availability for targeted degradation of sulfadiazine. Sep Purif Technol 299:121814. https://doi.org/10.1016/j.seppur.2022.121814

Li Y, Taggart MA, McKenzie C, Zhang Z, Lu Y, Pap S, Gibb S (2019) Utilizing low-cost natural waste for the removal of pharmaceuticals from water: mechanisms, isotherms and kinetics at low concentrations. J Clean Prod 227:88–97. https://doi.org/10.1016/j.jclepro.2019.04.081

Liu X, Liu Y, Lu S, Guo W, Xi B (2018) Performance and mechanism into TiO_2/Zeolite composites for sulfadiazine adsorption and photodegradation. Chem Eng J 350:131–147. https://doi.org/10.1016/j.cej.2018.05.141

Long M, Brame J, Qin F, Bao J, Li Q, Alvarez PJJ (2016) Phosphate changes effect of humic acids on TiO_2 photocatalysis: from inhibition to mitigation of electron-hole recombination. Environ Sci Technol 51(2016):514–521. https://doi.org/10.1021/acs.est.6b04845

Manjunath S, Kumar SM, Ngo HH, Guo W (2017) Metronidazole removal in powder-activated carbon and concrete-containing graphene adsorption systems: estimation of kinetic, equilibrium and thermodynamic parameters and optimization of adsorption by a central composite design. J Environ Sci Health Part A 52:1269–1283. https://doi.org/10.1080/10934529.2017.1357406

Maryam B, Mohammad MP, Elnaz D, Mohammad JD, Mohsen A, Shahriar O, Amir R, Mika S, Mahdieh D, Mohammad A (2022) Application of photo-fenton, electro-fenton, and photo-electro-fenton processes for the treatment of DMSO and DMAC wastewaters. Arab J Chem 15:104229. https://doi.org/10.1016/j.arabjc.2022.104229

Metcalfe CD, Bayen S, Desrosiers M, Muñoz G, Sauvé S, Yargeau V (2022) An introduction to the sources, fate, occurrence and effects of endocrine disrupting chemicals released into the environment. Environ Res 207:112658. https://doi.org/10.1016/j.envres.2021.112658

Michael I, Rizzo L, McArdell CS, Manaia CM, Merlin C, Schwartz T, Dagot C, Fatta-Kassinos D (2013) Urban wastewater treatment plants as hotspots for the release of antibiotics in the environment: a review. Water Res 47:957–995. https://doi.org/10.1016/j.watres.2012.11.027

Möhler JS, Kolmar T, Synnatschke K, Hergert M, Wilson LA, Ramu S, Elliott AG, Blaskovich MAT, Sidjabat HE, Patersonc DL, Schenk G, Cooper MA, Ziora ZM (2017) Enhancement of antibiotic-activity through complexation with metal ions–combined ITC, NMR, enzymatic and biological studies. J Inorg Biochem 167:134–141. https://doi.org/10.1016/j.jinorgbio.2016.11.028

Naghibi S, Hosseini HRM, Sani MAF (2013) Colloidal stability of dextran and dextran/poly ethylene glycol coated TiO_2 nanoparticles by hydrothermal assisted sol–gel method. Ceram Int 39:8377–8384. https://doi.org/10.1016/j.ceramint.2013.04.018

Pan S, Yan N, Liu X, Wang W, Zhang Y, Liu R, Rittmann BE (2014) How UV photolysis accelerates the biodegradation and mineralization of sulfadiazine (SD). Biodegradation 25:911–921. https://doi.org/10.1007/s10532-014-9711-4

Rong SP, Sun YB, Zhao ZH (2014) Degradation of sulfadiazine antibiotics by water falling film dielectric barrier discharge. Chin Chem Lett 25:187–192. https://doi.org/10.1016/j.cclet.2013.11.003

Sarode S, Upadhyay P, Khosa MA, Mak T, Shakir A, Song S, Ullah A (2019) Overview of wastewater treatment methods with special focus on biopolymer chitin-chitosan. Int J Biol Macromol 121:1086–1100. https://doi.org/10.1016/j.ijbiomac.2018.10.089

Shamsuddin N, Das DB, Starov VM (2015) Filtration of natural organic matter using ultrafiltration membranes for drinking water purposes: circular cross-flow compared with stirred dead end flow. Chem Eng J 276:331–339. https://doi.org/10.1016/j.cej.2015.04.075

Shymanovska VV, Khalyavka TA, Manuilov EV, Gavrilko TA, Aho A, Naumov VV, Shcherban ND (2022) Effect of surface doping of TiO_2 powders with Fe ions on the structural, optical and photocatalytic properties of anatase and rutile. J Phys Chem Solids 160:110308. https://doi.org/10.1016/j.jpcs.2021.110308

Shi Y, Hu Y, Wang Y, Li X, Xiao C, Liu J, Chen Y, Cheng J, Zhu X, Wang G, Xie J (2022) 3D *N*-doped graphene aerogel sponge-loaded CoS_2 co-catalytic Fenton system for ciprofloxacin degradation. J Clean Prod 380:135008. https://doi.org/10.1016/j.jclepro.2022.135008

Silva CP, Pereira D, Calisto V, Martins MA, Otero M, Esteves VI, Lima DLD (2021) Biochar-TiO_2 magnetic nanocomposites for photocatalytic solar-driven removal of antibiotics from aquaculture effluents. J. Environ. Manag. 294:112937. https://doi.org/10.1016/j.jenvman.2021.112937

Tanggg A, Dahmane M, Belabed C, Bellal B, Trari M, Richard C (2020) Photocatalytic degradation of quinoline yellow over Ag_3PO_4. Catalysts 10:1461. https://doi.org/10.3390/catal10121461

Wang N, Li X, Yang Y, Zhou Z, Shang Y, Zhuang X (2020) Photocatalytic degradation of sulfonamides by Bi_2O_3-TiO_2/PAC ternary composite: mechanism, degradation pathway. J. Water Process Eng. 36:101335. https://doi.org/10.1016/j.jwpe.2020.101335

Xiao Y, Zhang L, Zhang W, Lim KY, Webster RD, Lim TT (2016) Comparative evaluation of iodoacids removal by UV/persulfate and UV/H_2O_2 processes. Water Res 102:629–639. https://doi.org/10.1016/j.watres.2016.07.004

Xu W, Zhang G, Li X, Zou S, Li P, Hu Z, Li J (2007) Occurrence and elimination of antibiotics at four sewage treatment plants in the Pearl River Delta (PRD). South China Water Res 41:4526–4534. https://doi.org/10.1016/j.watres.2007.06.023

Yadav MSP, Neghi N, Kumar M, Varghese GK (2018) Photocatalytic-oxidation and photo- persulfate-oxidation of sulfadiazine in a laboratory-scale reactor: analysis of catalyst support, oxidant dosage, removal-rate and degradation pathway. J Environ Manag 222:164–173. https://doi.org/10.1016/j.jenvman.2018.05.052

Yang G, Mo S, Xing B, Dong J, Song X, Liu X, Yuan J (2020) Effective degradation of phenol via catalytic wet peroxide oxidation over *N*, *S*, and Fe-tridoped activated carbon. Environ. Pollut. 258:113687. https://doi.org/10.1016/j.envpol.2019.113687

Yang G, Chen H, Qin H, Feng Y (2014) Amination of activated carbon for enhancing phenol adsorption: effect of nitrogen-containing functional groups. Appl Surf Sci 293:299–305. https://doi.org/10.1016/j.apsusc.2013.12.155

Yao Y, Chen H, Lian C, Wei F, Zhang D, Wu G, Chen B, Wang S (2016) Fe Co, Ni nanocrystals encapsulated in nitrogen-doped carbon nanotubes as Fentonlike catalysts for organic pollutant removal. J Hazard Mater 314:129–139. https://doi.org/10.1016/j.jhazmat.2016.03.089

Yuan W, Cheng L, An Y, Lv S, Wu H, Fan X, Zhang Y, Guo X, Tang J (2018) Laminated hybrid junction of sulfur-doped TiO_2 and a carbon substrate derived from Ti_3C_2 MXenes: toward highly visible light-driven photocatalytic hydrogen evolution. Adv Sci 5:1700870

Zhang QQ, Ying GG, Pan CG, Liu YS, Zhao JL (2015) Comprehensive evaluation of antibiotics emission and fate in the river basins of china: source analysis, multimedia modeling, and linkage to bacterial resistance. Environ Sci Technol 49:6772–6782. https://doi.org/10.1021/acs.est.5b00729